Computer Study of Atomic Mechanisms of Intercalation/ Deintercalation of Li Ions in a Silicene Anode on an Ag (111) Substrate

Alexander Y. Galashev [z] and **Ksenia A. Ivanichkina**

Institute of High-Temperature Electrochemistry, Ural Branch, Russian Academy of Sciences, Yekaterinburg 620990, Russia

The ability of silicon to hold a large amount of lithium puts silicene in a series of the most promising materials for the anode of lithium-ion batteries. An increase in the rate of movement of lithium ions through silicene can be achieved with silicene having vacancy-type defects. The effect of vacancy-type defects on the fill ability with lithium of the channel formed by silicene sheets on the Ag (111) substrate, as well as on the structural and kinetic properties of lithium, has been studied by the molecular dynamics method. The limit number of intercalated lithium atoms and their self-diffusion coefficient increase with the transition from the perfect silicene channel to the channel containing mono- and bivacancies. The lithium structure in the channel was studied using the method of statistical geometry. The packing of the lithium atoms in the channel turns out to be partially ordered due to the regular placement of some of the atoms at their fixation opposite the centers of hexagonal Si-cells. The σ_{zz} stress in the sheets of silicene decreases during intercalation of lithium and increases at the final stage of deintercalation.
© 2018 The Electrochemical Society. [DOI: 10.1149/2.0751809jes]

Silicon has now become a promising candidate for an anode material in lithium-ion batteries (LIBs). Silicon has a theoretical charge capacity of 4200 mAhg^{-1} when fully lithiated. Silicon can obtain such high values of charge capacity due to the number of lithium atoms that can be alloyed in silicon, the fully lithiated alloy is Li$_{4.4}$Si.[1] As lithium atoms are added to the silicon lattice, the lattice will expand. Once the complete alloy is formed, the new fully lithiated alloy will have a fourfold increase in volume as compared to the original silicon lattice.[2] This volumetric expansion can cause severe cracking and ultimately failing of the silicon anode due to the loss of electrical contact. One way of improving the cycle performance of silicon is to reduce the size of the particles that are used in the anode. The size reduction helps to control the volume change and stresses in the Si. A thin film with a small thickness (about 50 nm) can have extremely high specific charge capacities, however will eventually fail from the stresses caused by lithiation and delithiation.[3] While thin films show the highest charge capacity, they offer the lowest number of cycles. In its turn, composite binder structures have the highest number of cycles, but the added weight greatly reduces the effective specific charge capacity.

Silicene–the silicon-based counterpart of graphene–has a two-dimensional structure that is responsible for the variety of unique chemical and physical properties. The existence of silicene has been achieved recently owing to experiments involving the epitaxial growth of silicon as stripes on Ag(001), ribbons on Ag(110), and sheets on Ag(111). If a 50-nm thick silicon film were formed by the addition of silicene sheets, then the number of such layers would be in the order of 100. Adsorption and desorption of lithium on silicene does not lead to an irreversible change in its structure. At the same time, the extremely high capacitive properties of the two-dimensional modification of silicon are retained. Therefore, the anode formed by stacked silicene sheets is a promising construction. It gives a high capacity and is stable during cycling. On the one hand, the interstices between the silicene sheets must be sufficient for the free penetration of lithium atoms, and on the other hand, their magnitude cannot be too large, since Lithium should be retained in the gap after charging the battery.

This anode design only partially eliminates the problem associated with the lack of porosity in a continuous multilayer silicon film. The lack of porosity leaves no room for the volumetric expansion that will occur during lithiation. This will lead to a buildup of stresses that will eventually crack the film. Once the film cracks too much, lithium ions will not cycle properly. To increase the rate of displacement of lithium ions within the anode, silicene sheets permeable to ions should be used. In other words, the anode can be constructed from silicene sheets having vacancy defects. However, the presence of defects in the sheets of silicene reduces their strength, which can lead to the destruction of the anode during the cycling process. In this connection, it is necessary to investigate both the penetrating ability of ions during their movement through porous silicene membranes, and to have an idea of the distribution of stresses in membranes.

The longitudinal and transverse motion of single lithium ions in flat channels formed by sheets both perfect and defective graphene was investigated in Refs. 4–6. An analogous study was also carried out for plane silicene channels, including in the presence of defects in silicene sheets.[7–9] However, based on these studies, one cannot judge the effect produced by a large number of lithium atoms penetrating into the silicene channels.

Silicene anodes can be constructed only in the presence of a substrate. The simplest way is to make an anode on the same substrate on which the silicene was obtained. The main substrates for the production of silicene are still silver substrates, and silicene sheets are obtained on an Ag (111) substrate. Thus, as the object of investigation, we chose a two-layer silicene, which is located on an Ag (111) substrate.

The silicon enables long life and high-energy storage, resulting in a significantly longer lasting battery. In the anode structure under consideration during charging the lithium ions fit into the gaps between the silicene sheets–a process known as intercalation. Penetrating into the anode, the Li$^+$ ion quickly acquires an electron and becomes a neutral atom. In the course of the reverse process (deintercalation), the Li atoms discharge electrons and, in the form of ions, rush to the cathode. The vast majority of available lithium-ion batteries consist of two electrodes connected by a liquid electrolyte. This electrolyte makes it difficult to reduce the size and weight of the battery. Additionally, they are subject to leakage so that the lithium in the exposed electrodes then encounters with oxygen in the air and undergoes self-ignition. Optimization of the liquid electrolyte composition to extend the LIB life remains challenging. LiPON, lithium phosphorus oxynitride, is an amorphous glassy material that can be used as an electrolyte material in thin film lithium-ion batteries.

The purpose of this study is to investigate the processes of intercalation and deintercalation of lithium ions occurring in a plane silicene channel, as well as determination of the kinetic properties of the Li ions and atoms in a channel, and investigation of the effect of defects on stress distribution in lithiated silicene sheets on the Ag (111) substrate.

Materials and Methods

Lithium ions are efficiently transferred and electronically isolated in a lithium-ion battery. The scheme of a typical
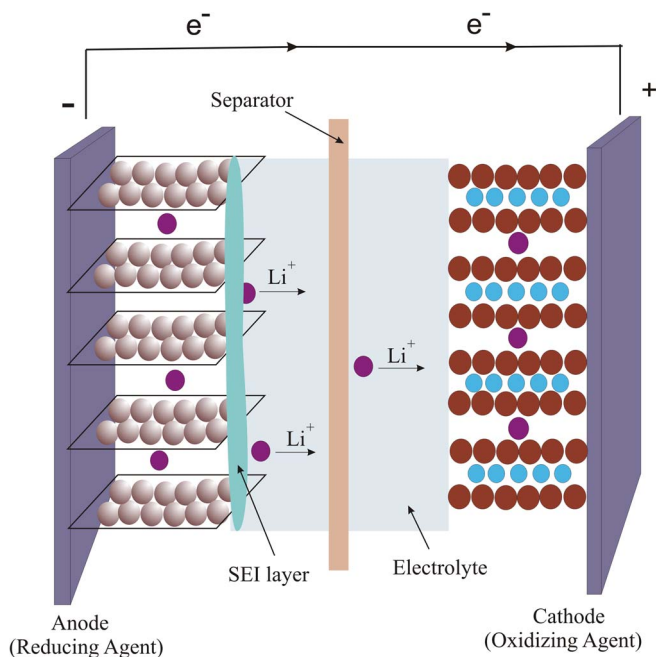
^{z}E-mail: galashev@ihte.uran.ru

Figure 1. Schematic of a typical state-of-art lithium-ion battery.

Table I. Parameters of Tersoff potential for silicon.

Parameters	Unit	Value
A	eV	1830.8
B	eV	471.18
λ_1	nm^{-1}	2.4799
λ_2	nm^{-1}	1.7322
n		0.78734
c		$1.0039 \cdot 10^5$
d		16.217
$R^{(1)}$	nm	0.27
$R^{(2)}$	nm	0.30
β		$1.1 \cdot 10^{-6}$
h		-0.59825

from it by pairs. When two ions are introduced into the channel simultaneously, the distance between them was no less than 1 nm. In this case, the interaction energy between two point elementary charges was no more than 1.44 eV. The work on moving an elementary point charge over a distance of 1 nm along the field force line exceeded this value by more than 2.5 times and was equal to 3.69 eV. The binding energy of lithium with silicene is ~2.2 eV per Li atom and shows small variation with respect to Li content while the barriers for Li diffusion are relatively low, typically less than 0.6 eV.[7] The results of the molecular dynamics simulation performed with the selected potentials indicate the adequacy of the model used.[7–9] The height of the silicene buckle Δh and the Si−Si bond-length $\bar{L}$ can vary for various reasons. For example, due to the interaction of silicene with the substrate, the presence of defects (especially large ones) in the silicene, the interaction of silicene with ad atoms and metal ions, etc. In the present simulation of lithium adsorption on silicene, the value of Δh increases from 0.64 (for perfect silicene) to 1.44 Å (for silicene with trivacancies) and the value of $\bar{L}$ changes from 2.30 to 2.44 Å. These values of $\bar{L}$ agree well with the values of the average Si-Si bond length for Si$_{400}$ nanoparticles in the vitrified (0.242 nm) and amorphous state (0.236 nm).[15] The calculated adsorption energy for lithiated silicene ranges from 2.27 to 2.52 eV / Li (depending on the location of the Li atom). The average length of the Si-Li bond is 0.265 nm, which agrees well with the data of Ref. 16.

In this paper, we consider the case of the 4 × 4 surface reconstruction. The unit cell of a silicene structure contains 18 Si atoms. Six atoms of the unit cell are displaced by the distance of 0.064 nm perpendicular to the surface and the other Si atoms are on the same (original) plane. Such a structure is similar to an arrangement of the silicene surface observed on the Ag (111) substrate.[17] If atoms protruding above the original surface in the top-sheet of the two-layer silicene are displaced upwards such atoms of the lower sheet stayed down. Various periodic structures are observed for silicene on Ag (111) such as 4 × 4, $(2\sqrt{3}\times2\sqrt{3})$R30°, $(\sqrt{7}\times\sqrt{7})$R19.1°, and $(\sqrt{13}\times\sqrt{13})$R13.9°.[18–20] Almost all experimental studies confirm that Si atoms in silicene form a buckled honeycomb lattice. We apply the 4 × 4 model of silicene, since its validity was confirmed by various experimental methods including non-contact atomic force microscopy,

lithium-ion battery with liquid electrolyte is shown in Figure 1. To improve the battery liquid solvent and polymer separator should be replaced by the solid electrolyte. When using silicene on a metal substrate as an anode material, the metal part of this structure should not directly connect to an external electrical circuit, i.e. contact with the circuit must be carried out only through silicene. In addition, the metal substrate must be isolated from the electrolyte. Metal (in this case Ag) is present only because silicene cannot be separated from it. Although the presence of an Ag substrate can increase the electron transfer rate to Li$^+$ from silicene. In lithium-ion batteries, capacity fade occurs over thousands of cycles, limited by slow electrochemical processes, such as the formation of a solid-electrolyte interphase (SEI) in the negative electrode, which compete with reversible lithium intercalation. Rapid degradation is often the limiting factor in developing new electrode materials but practical Li-ion batteries necessarily exhibit slow degradation over hundreds or thousands of cycles. Such slow capacity fading usually arises from irreversible electrochemical processes. Initially, SEI formation protects the electrode against solvent decomposition at large negative voltage, but over time, it leads to a gradual capacity fade as the SEI layer thickens. However, the formation of SEI is not the only problem when finding new anode materials for LIB. It is very important to know how thin-film silicon materials on substrates will behave themselves when intercalating with lithium. A theoretical understanding of the processes occurring at the anode will assist the design of high-performance batteries. The model used in the theoretical analysis should be as simple as it can be without neglecting important effects.

The calculations were performed by classical molecular dynamics (MD). Tersoff potential with the parameters of Ref. 10 was taken to represent the interactions in silicene. The Tersoff potential parameters are shown in Table I. The interaction between Si belonging to different sheets of silicene is described by Morse potential.[11] The Li-Li, Li-Si, Li-Ag, and Si-Ag interactions were presented by Morse potential too.[12–14] Parameters of the Morse potentials under consideration are listed in Table II. The silver substrate was formed by four (111) planes of the corresponding crystal and contained 1120 atoms (4 layers of atoms). Atoms of the substrate were immobile, so Ag-Ag interaction was not considered in the model. The electric field acted only on the Li$^+$ ions, having an electric charge 1e, where e is an elementary electric charge. The coulomb interaction acted between two lithium ions when they were introduced into the channel or were removed

Table II. Parameters of Morse potential describing various interactions.

Interaction*	D_0 (meV)	α (nm^{-1})	r_m
Si$^{(1)}$ − Si$^{(2)}$	227.40	44.992	0.154
Li − Li	420.76	7.899	0.300
Li − Si	309.30	36.739	0.116
Li − Ag	373.92	30.570	0.108
Ag − Si	274.89	14.540	0.374

*The upper indexes at Si denote the belonging to the layer of atoms 1 or 2.

scanning tunneling microscopy, angle-resolved photoelectron spectroscopy, and low-energy electron diffraction.[17] In addition, atomic structure of the monolayer 4×4 silicene occupies the largest part of the surface of epitaxial silicene on the substrate Ag (111).[21] During the entire calculation, the average height of the protrusions produced by the Si atoms in the model was kept with a good degree of accuracy. A slight difference (<0.005 nm) in the height of the buckles as well as the horizontal dimensions of the reconstruction determined by different models of silicene obviously cannot greatly affect the result of the simulation. Simulation shows that the gap h_g between the silicene sheets has a major effect on the motion of ions in the channel. It is the value of h_g and the electric field strength that determine the channel capacity.

The estimated concentrations of mono- and bi-vacancies in silicene obtained on Ag (111) can be quite high such as 4.4×10^{13} cm^{-2} and 5.0×10^{13} cm^{-2} respectively.[22] It means that there would be one defect in every 2 nm^2 area. The large concentration of point defects together with easy diffusion and coalescence of vacancy defects nicely explains a low stability of silicene in experiments.

In the case of the Li$^+$ ion movement in the flat channel under the action of the longitudinal electric field the gap was $h_g = 0.75$ nm wide. It was previously determined that for such a gap size the single Li$^+$ ion can be in a silicene channel during 100 ps in the presence of an electric field of 10^3 V / m.[7] Perfect silicene sheet had a size of 4.8×4.1 nm (taking into account the size of Si atoms) and contained 300 atoms. Nine similar defects in form of single vacancies and bi-vacancies were created approximately evenly with a displacement of 0.1–0.2 nm in each (x and y) direction for different silicene sheets. The silicene sheet contained 291, 282 atoms in each of these cases. Silicene sheets were arranged in accordance with the stacking of Bernal (ABAB . . .) in exactly the same way as graphene sheets in graphite.[23] Securing the sheet edges of silicene creates conditions for preserving the morphology of porous silicene. The numerical solution of the motion equations was performed by the Runge-Kutta method of order 4 with the time step of $\Delta t = 1 \times 10^{-16}$ seconds.

In classical molecular dynamics, empirical interaction potentials are used that remain unchanged throughout the calculation, in addition, the number of particles in the model should also remain unchanged. In this case, the thermodynamic and kinetic properties of the system can be correctly calculated. Since it is important for us to calculate these properties, we choose the length of one MD calculation to be equal to 100000 time steps or 10 ps. Such a length of MD calculation is sufficient to calculate the equilibrium properties (total energy and stress tensor) of the system and the self-diffusion coefficients of the atoms. The next MD calculation was carried out with a changed number of particles in the model. When studying intercalation of lithium, the number of particles increased by 1 or 2 Li$^+$ ions, and in the simulation of deintercalation in each subsequent calculation, the system had 1 or 2 Li atoms less than in the previous calculation. In addition, an interval of 10 ps was sufficient to allow an ion or two ions to find energetically advantageous places in the channel and stay in them.

The standard codes of the LAMMPs program allow calculations to be made until all the particles in the system are in a predetermined confined space. Calculations cease if at least one of the particles leaves this space. In order that this does not happen, the investigated functioning model of the silicene electrode is placed in a rectangular container. Moreover, at the initial instant of time, the distance from any Si atom belonging to the boundary of the silicene sheets or the Ag atom to the nearest wall of the container was not less than 0.5 nm. The distance from the Si atoms of the top sheet of the silicene to the top wall of the container was 1.15 nm. The interaction of Li$^+$ ions (or Li atoms) with the wall occurred only when they approached the wall at a distance $r < R_{cutoff} = 0.25$ nm. The distance from the atom (ion) to the wall was determined from the perpendicular. A lithium atom (or ion) could interact with the container wall according to the Lennard-Jones potential (12–6) with parameters $\sigma = 0.1$ nm, $\varepsilon = 1$ eV. These parameters are not relevant to any real material and are chosen empirically to obtain an adequate model for filling the silicene

channel. If the distance to the wall was less than 0.1 nm, a repulsive force acted on the atom (ion) from the side of the wall, and eventually its motion changed to the opposite, i.e. it began to move back to the system.

In our earlier calculations, it was shown that the value of the electric field strength of 10^3 V/m is optimal for rapid jump-like diffusion of an ion in a silicene channel with a gap of 0.75 nm.[7] It should be noted that for a constant electric field with an intensity of 10^3 V / m, the lithium ion completely passes flat graphene channels with a gap of 0.60 and 0.65 nm and a length of ~4 nm.[4,5,23] Approximately such an electric field strength is achieved by using the LiPON film with thickness of ~30 micron as a solid electrolyte to create a working voltage of 1.5 V in the LIB.[24] To observe a similar effect in the silicene channel having a length of 4.7 nm, it was necessary to increase the gap width to 0.75 nm and the electric field to 10^4 V/m.[7–9] The lithium ion migrates along such a channel and at the electric field strength of 10^3 V / m, but it cannot overcome the energy barrier to exit the channel in this case.

Calculation

Simulation of the intercalation process consisted in the periodic single or double emission of Li$^+$ ions from points with random y coordinates on a line having constant coordinates $x = 0.198$ nm, $z = 0.375$ nm. In other words, the line of initial points was near the channel entrance with a slight shift inward at a height $h_g/2$. The ends points of the line were inside the channel at a distance of 0.2 nm from the coordinates of the extreme silicene atoms, which limit the extent of the sheets along the y direction. The ion moved under the action of a constant electric field with a strength of 10^3 V / m during 100,000 time steps. In the case of a uniform lifetime (10 ps), the ion succeeds in finding an advantageous location on the surface of the silicene and staying there until the end of the time allotted to it. The ion was not have had this opportunity if the lifetime was a stochastic variable.

Until the maximum filling of the channel with lithium, the ion remained in the channel during the entire lifetime (10 ps), mainly because it could not overcome the barrier created by the attracting interaction of other atoms. When a lithium ion is converted to a Li atom (after a set time of 10 ps), the nature of its interaction with other atoms (Si and Li) did not change, but the electric field no longer had any influence on it. In other words, the transition of the Li$^+$ ion to an atom meant a change in its electric charge from +1 to 0 (every 10 ps), which did not affect its interactions not related to the presence of an electric charge. After every 10 ps, a new Li$^+$ ion was launched into the channel. This procedure was repeated until the ions could find a place in the channel. The limiting number of intercalated lithium atoms turned out to be 39 in the case of a channel from a perfect silicene. All attempts to increase the number of Li atoms above this value were unsuccessful, since the Li$^+$ ion eventually either left the channel outward, or did not enter in the channel at all. For the channels formed by the defective silicene, intercalation and deintercalation were carried out by inserting ion pairs into the channel and removing them from it, respectively. At the end of the intercalation, we obtained a system in which electrically charged particles (ions) are completely absent.

During deintercalation, charged particles were again present in the system: one ion in the case of a channel formed by perfect silicene or silicene with monovacancies and two ions for a channel with silicene walls having bivacancies. The process of deintercalation of lithium was carried out when the direction of the electric field was reversed and the modulus of this magnitude was increased to 10^4 V / m. The order of appearance of ions in the system also had an inverse order, i.e. the last of Li$^+$ ions that got into the channel became the first one, etc. The lifetime of the ion remained the same, i.e. was 10 ps. Ion always left the channel during its lifetime and left the channel without the accompaniment of lithium atoms. It was established in a separate series of calculations that such a character of the inverse process is not related to the order in the sequence of conversion of atoms into ions. It was shown that a change in the order of the exit of ions from the channel did not lead to any new result. So when the choice of

the outgoing ions was made randomly, each ion came out from the channel alone without the accompaniment of other atoms.

Self-diffusion coefficient was calculated by the mean square displacement of the atoms $\langle [\Delta \mathbf{r}(t)]^2 \rangle$

$$D = \lim_{t \to \infty} \frac{1}{2\Gamma t} \left\langle [\Delta \mathbf{r}(t)]^2 \right\rangle, \qquad [1]$$

where $\Gamma = 3$ is dimension of the space, the $\langle ... \rangle$ angle brackets denote averaging over time.

To calculate stresses appearing in silicene, silicene sheets were subdivided into surface elements. The stresses $\sigma_{u\alpha}(l)$ produced by the action of forces of the α (x, y, z) direction are computed on each surface element with a number l and of orientation u. In these calculations, use was made of the products of the projections of atomic velocities and the projection of the forces f_{ij}^{α} acting on the lth element from the other atoms in the case of observance of the relevant conditions[25]

$$\sigma_{u\alpha}(l) = \left\langle \sum_i^n \frac{1}{\Omega} \left(m v_u^i v_\alpha^i \right) \right\rangle + \frac{1}{S_l} \left\langle \sum_i^n \sum_{j \neq i}^{(u_i \leq u, u_j \geq u)} \left(f_{ij}^{\alpha} \right) \right\rangle. \qquad [2]$$

Here k is the number of atoms on the lth element, Ω is the volume per atom, m is the atomic mass, v_α^i is the α projection of the velocity of the ith atom, S_l is the area of the lth element (the force resulting from the interaction of i and j atoms and passes though the lth element), and u_i is the running coordinate of the atom i; the symbol u in the superscript of the sum denotes the coordinate of the contact point of the straight line through the centers of the atoms i and j and the lth surface element.

Structural analysis of small objects can be carried out using the statistical geometry method based on the construction of the Voronoi polyhedra (VPs).[26] In the case of polyatomic system, atoms of one type may play the role of polyhedron centers, while atoms of another type may serve as their nearest neighbors that determine the polyhedron faces. For example, in the case of the "Li-silicene channel" system, it is advantageous to use lithium atoms as the centers and select the nearest neighbors among Si atoms. These hybrid polyhedra are easier to construct, since the number of Si atoms is greater than of Li atoms. However, in this case hybrid polyhedra are not Voronoi polyhedra, since they fail to fill completely all of the space occupied by molecules without voids and overlaps. VP faces determine the cyclic structures formed from Li atoms, while hybrid polyhedra faces determine rings composed of Si atoms. However, there is still a way to construct Voronoi polyhedra in a multicomponent system, when the dimensions of all atoms the same. And we will not take into account the difference in the sizes of Li and Si atoms in the construction of VP, and we will construct VP for Li atoms when the geometric neighbors are Li and Si atoms together or only Li atoms.

A modified LAMMPS code for parallel computing in the applied MD method was used.[27] Fragments were introduced in the program to calculate kinetic and mechanical properties of the system. The calculations were performed on a hybrid cluster calculator "Uran" at IMM UB RAS with a peak performance of 216 Tflop / s and 1864 CPU.

Results and Discussion

The configuration of the "Ag-Si-Li" system, referring to a time point of 390 ps at the final filling by lithium of the channel formed by sheets of perfect silicene, is shown in Figure 2. During this time, 39 lithium ions were introduced into the channel. All intercalated Li atoms are visible in the figure, because silicene sheets are shown as transparent. It is seen that not all Li atoms are adsorbed by silicene. Four Li atoms were found outside the channel, one of which is found at a considerable distance from the lower sheet of silicene. It is clear that in the process of deintercalation, each of these atoms, turning into an ion, freely leaves the system. At the same time, external Li atoms will not affect the location of other lithium atoms in the channel. In addition, the arrangement of these four atoms is such that they cannot
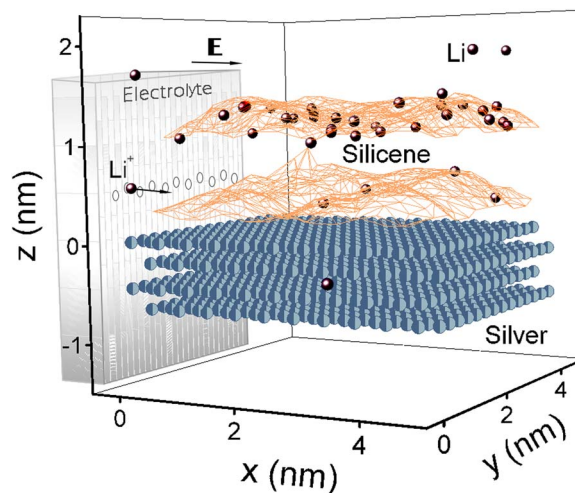

Figure 2. Silicene channel, formed by perfect silicene sheets, on the substrate Ag (111) after the intercalation process with lithium.

interfere with the escape of other ions from the channel during deintercalation. Therefore, the four Li atoms located outside the channel were removed from the system before the deintercalation process began. The procedure for liberation from the "extra" Li atoms was also carried out for silicene channels containing mono- and bivacancies. In these cases, prior to deintercalation, 5 and 15 Li atoms were removed from the system for channels with mono- and bivacancies, respectively. As can be seen from Figure 2, the overwhelming majority of Li atoms are adsorbed by the top sheet of silicene. This is the result of the influence of the metal substrate, since in the absence of a substrate the number of adsorbed Li atoms by each silicene sheet is approximately equal.

The limiting filling of the channel with lithium led to the highest height of the dome formed by the upper sheet of silicene. The highest dome was formed for sheets of perfect silicene. The deformation of silicene sheets leads to an increase for space available for filling the channel with lithium, which in the case of perfect silicene reached 45%. Strong deformations of silicene sheets on the Ag (111) substrate contribute to the structural rearrangement of vacancy-type defects in silicene. For sheets of silicene with defects, the magnitude of the vertical deformation was reduced as well as the volume of the inter-sheet space decreased. The horizontal (along the axis ox) and the vertical (along the axis oz) profiles of lithium density in the silicene channel are usually of the same type for both perfect silicene sheets and sheets with various vacancy-type defects. For example, Figure 3 shows the corresponding profiles of numerical density in the case of presence of bi-vacancies in silicene. The values of x and z are calculated from the entrance to the channel (x = 0) and from the level of the lower sheet of silicene (z = 0). In this case, 64% of all Li atoms are more "tied" to the upper sheet and only 36% to the lower one. Depending on the size of the defects, from 15 to 40% of Li atoms "adjoin" to the lower sheet of silicene lying on the Ag (111) substrate, and from 60 to 85% to the upper one. The range of the distribution of Li atoms along the z coordinate is much larger than the initially specified interval between the silicene sheets (0.75 nm). This is due not only to the strong deformation of the silicene sheets, but also to the escape of individual Li atoms through the bivacancies beyond the sheets boundary. The region at the half-width level of the channel is free.

The use of Cu (111) substrates changed the lithium density profiles. In this case, the silicene channel is filled with lithium more homogeneously. The horizontal density profile indicates a significant fraction of Li atoms concentrated near the entrance to and exit of the channel. The shape of the vertical density profile indicates that the middle part of the channel is not free, but is most densely filled with Li atoms. The Li atoms are not densely "adjacent" to the upper sheet of the
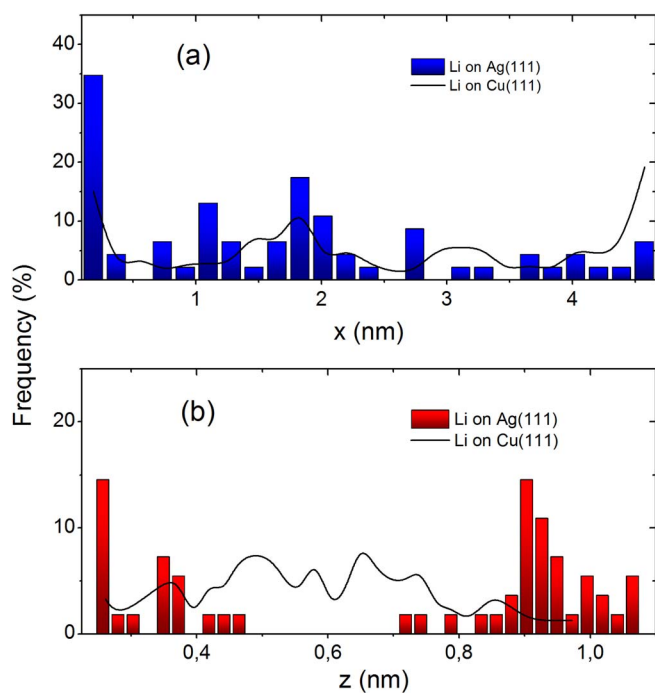
Figure 3. Horizontal (longitudinal) and vertical profiles of lithium density in a silicene channel with bivacancies on the Ag (111) and Cu (111) substrates.
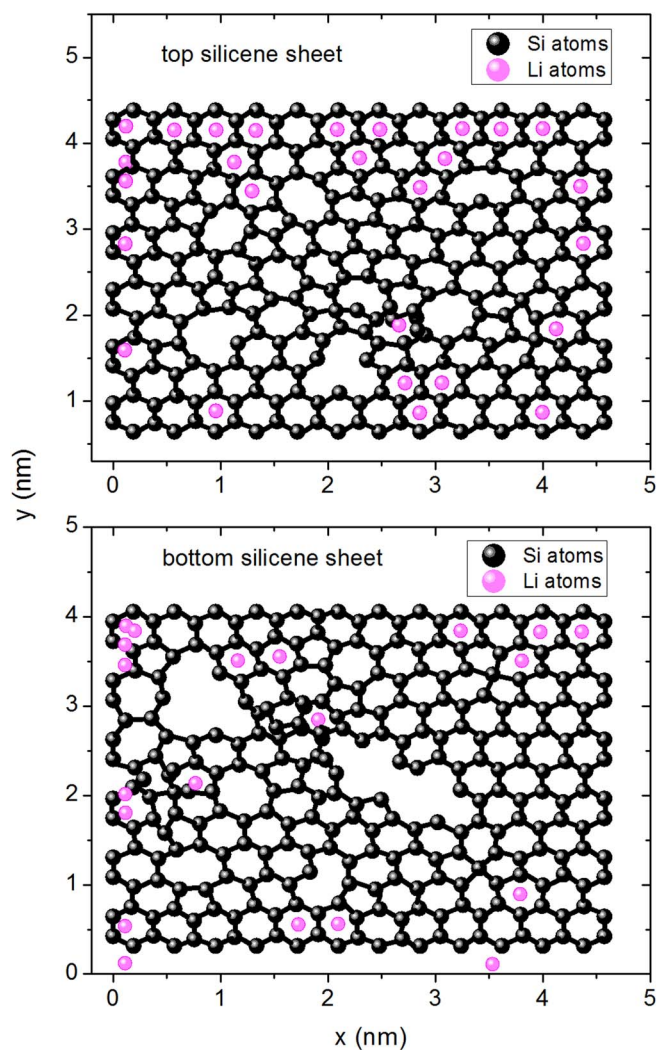

Figure 4. Xy-projections of the upper and lower sheets of silicene with monovacancies on the Ag (111) substrate, at the time of complete lithiation (51 lithium atom was adsorbed on the silicene surface).

silicene, leaving a small free gap near it. This is because there is a stronger attraction between the Cu and Li atoms than between the Ag and Li atoms. The results of MD simulations show that the vacancy defects are better preserved during lithiation in silicene located on the Cu (111) substrate than on the Ag (111) substrate.

Let us consider in more detail the behavior of defects and the attachment of Li atoms to silicene sheets by the example of a silicene channel having monovacancies and being fully filled with lithium. The investigated configurations refer to a time point of 0.51 ns (or 5.1×10^6 Δt). The xy-projections of the upper and lower layers of the channel cut by the mean ($z = h_g^*/2$) plane are shown in Figure 4 (view from the side of the plane $z = h_g^*/2$), where h_g^* is the vertical channel size after intercalation of lithium. In each sheet of silicene there are 8 cavities, the sizes of which exceed the size of any cavity formed by six-link rings. The bottom sheet contains the two largest cavities, the boundary of which is formed from 23 and 15 Si atoms. The two largest cavities of the top sheet are bounded by 13 and 10 Si atoms. Their size is significantly inferior to the size of the largest cavities of the bottom sheet, which is due to the interaction of this sheet with the substrate. There are 8 rings in each sheet, the number of links of which exceeds 6 and 12 five-link rings. The upper and lower parts of the channel have equal volumes, but the number of Li atoms in them is different: 27 Li atoms are in the upper part and 20 Li atoms are present in the lower part. Four Li atoms are outside the gap formed by silicene sheets and are not included in the *xy* channel projections.

The change in the specific internal energy $\langle U \rangle$ of lithium during the filling of the silicene channel with Li atoms is shown in Figure 5. The figure is divided into two parts by a dashed line. The left part of the figure shows the intercalation of lithium into the gap between the silicene sheets, and the right side of the figure reflects the reverse process of the lithium deintercalation. On each part of the figure, three graphs are presented, related to the silicene channels formed by defect-free silicene sheets, sheets with monovacancies and with bivacancies. The abscissa is the number of Li atoms in the channel. The limiting number of Li atoms intercalated into the channel increases in the sequence "defect less silicene → silicene with monovacancies → silicene with bivacancies". In all the cases considered, the intercalation

of the first 1–3 lithium atoms gives rise to a burst of energy $\langle U \rangle$. This is due to the structural perturbations produced by high-energy lithium ions (atoms) freely moving through the channel. With further increase of Li atoms in the channel due to their binding to Si atoms of the upper and lower sheets of silicene, the growth of the $\langle U \rangle$ value is replaced by its decrease.

The deformation of silicene sheets and their binding to lithium are factors acting on the $\langle U \rangle$ magnitude in different directions. Because of the rapid change in these events, the $\langle U \rangle$ magnitude undergoes strong fluctuations, which are manifested especially long when there are monovacancies in the silicene sheets. It is obvious that it is easier to deform the sheets of defective silicene than sheets of perfect silicene. However, when the silicene sheets contain bivacancies, the Li atoms bind to these defects more easily and are held by them. As a result, the $\langle U \rangle$ fluctuations in this case turn out to be minimal, but the "Si-Li" system as a whole proves to be more strongly disordered in comparison with the cases of perfect silicene and silicene with monovacancies. The minimum value $\langle U \rangle$ for saturation of the channel with lithium is observed for paired sheets of perfect silicene, and the maximum value for silicene sheets with bivacancies.

The deintercalation process is also accompanied by jumps of $\langle U \rangle$, but not as strong and rapid as during intercalation. These oscillations are mainly associated with the destruction of the Li structure in the silicene channel during deintercalation. In the case of a perfect silicene,
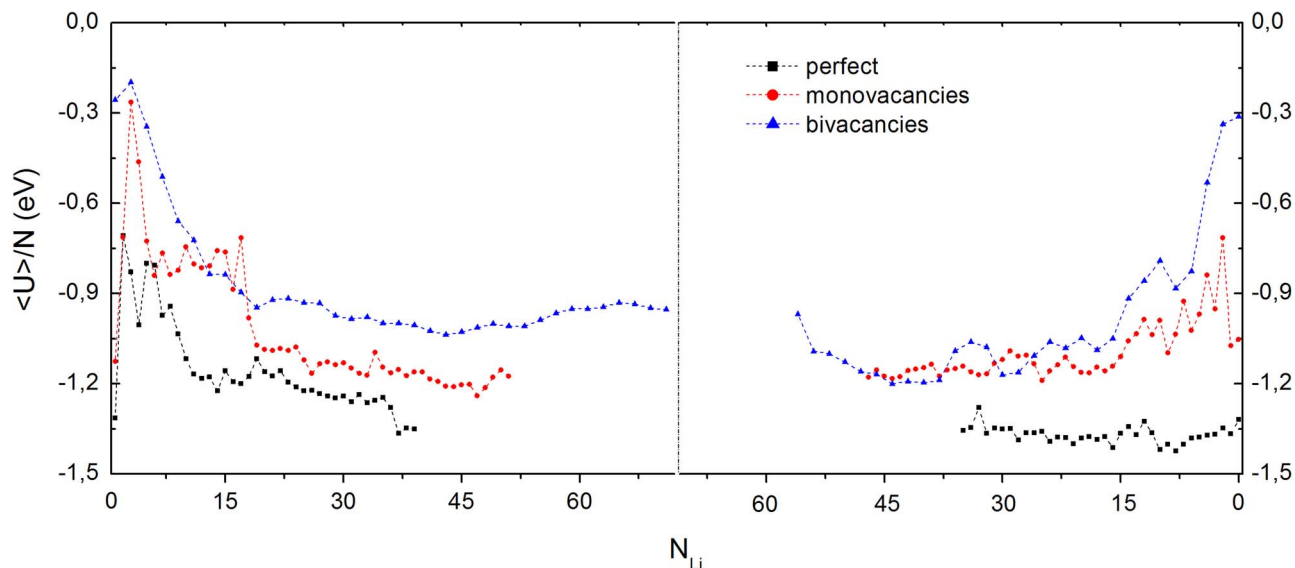
Figure 5. Internal energy of lithium atoms in the process of intercalation (left) and deintercalation (right) in various flat silicene channels. N_{Li} is the number of lithium atoms in the channel.

the $\langle U \rangle$ energy retained its low value after the channel was completely freed from lithium. However, when the silicene sheets have defects, the $\langle U \rangle$ value begins to increase after approximately 30 lithium ions are removed from the system, because the residence time of the ion in the channel increases. This makes it possible to disperse lithium ions in the channel by an applied electric field. The collision of a fast lithium ion with Li and Si atoms is even stronger than that in a period of unchanged energy $\langle U \rangle$. Such collisions destroy the structure of the "Si-Li" system and lead to an increase in the $\langle U \rangle$ magnitude.

The behavior of the D self-diffusion coefficient of Li atoms during intercalation and deintercalation of lithium ions into silicene channels is shown in Figure 6. Dependencies $D(N_{Li})$, where N_{Li} is the number of atoms Li in the channel, are presented for: (a) a flat perfect silicene channel; (b) a channel formed by silicene sheets with monovacancies; (c) a channel constructed from silicene sheets with bivacancies. The vertical line divides each of the figures (a) - (c) into the left and right parts. The left-hand parts of the figures represent the process of intercalation of lithium ions into the flat silicene channel, while the right-hand parts of these figures reflect the Li$^+$ ion deintercalation process. In the case of the channel formed by sheets of perfect silicene, the limiting number of Li atoms filling the channel was 39. The silicene channel with monovacancies was able to hold a maximum of 51 Li atoms, and the channel with bivacancies could contain no more than 71 Li atoms. In cases (a) and (b), lithium ions were intercalated and deintercalated one by one sequentially, while in case (c), sequential pair intercalation and deintercalation were simulated. In other words, in the case of (c), immediately two Li$^+$ ions entered the channel and emerged from it.

In each of the cases (a) - (c), the self-diffusion coefficient of Li atoms decreases as the channel is filled with these atoms. The strongest fluctuations of D magnitude are observed at the initial part of the channel filling with Li atoms, because here the Li$^+$ ion has a higher velocity, which it loses when colliding with Si and Li atoms. We note that the D value increases by an order of magnitude in both processes when passing from the channel formed by the perfect silicene, to the channel formed by silicene sheets with monovacancies or bivacancies. This is due not only to the achievement of greater freedom of movement in the presence of defects in the sheets of silicene, but also to the weakening of the interaction of the Li$^+$ ion with Si atoms in the presence of monovacancies, let alone bivacancies. The smoother attenuation of the coefficient fluctuations during intercalation of lithium ions in case (c) is due to the simultaneous action of two ions on the channel walls and on its contents.
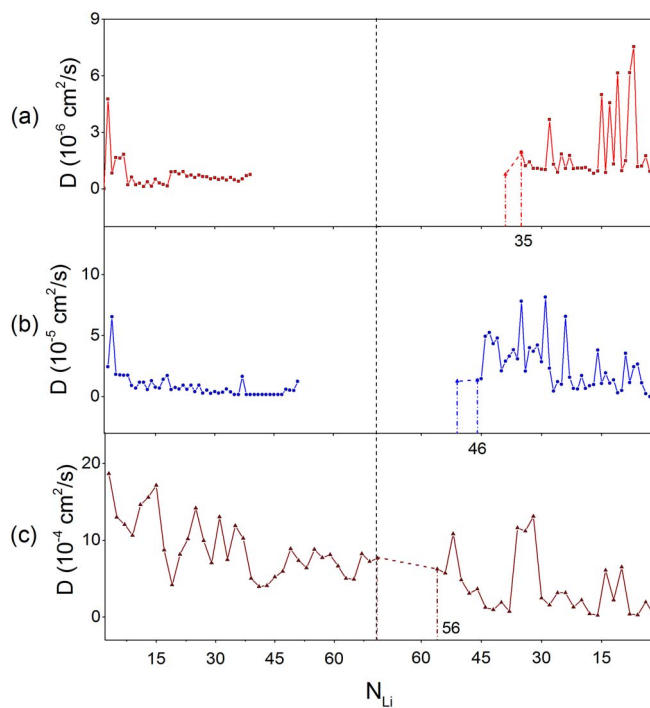

Figure 6. The coefficient of self-diffusion of lithium atoms in the process of intercalation (left) and deintercalation (right) in silicene channels characterized as: (a) perfect, (b) with monovacancies, (c) with bivacancies. Removal of the lithium atoms that are outside the channel before the start of deintercalation is marked in the figure by dashed lines and dot-dash lines.

In the cases (a) and (b) at the initial stage, Li$^+$ ion deintercalation occurs without large changes in the D coefficient of lithium atoms. However, when about a dozen or two dozen Li atoms leave the channel, the fluctuations in the D magnitude become large. This is due to an increase in the Li$^+$ ion velocity in the freer channel, and, consequently, also with its stronger collisions with Si and Li atoms. The paired exit of Li$^+$ ions from the channel in case (c) occurs without amplification of the D coefficient fluctuations at the final stage of deintercalation.
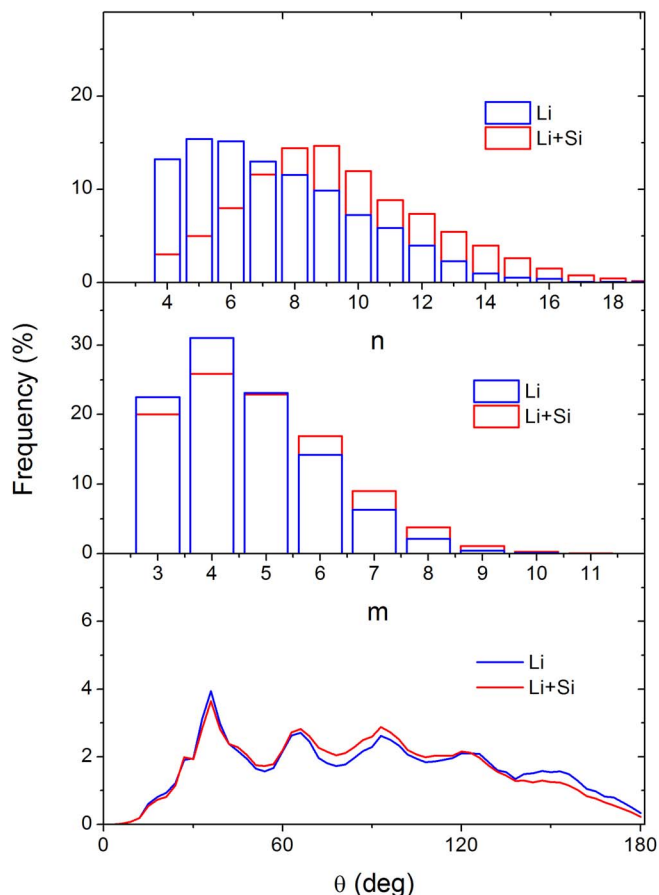
Figure 7. Distribution of VP with respect to the number of faces (n), distribution of faces by the number of sides (m) and distribution of angles (θ) formed by the nearest geometric neighbors. VP are constructed for Li atoms in the case when they completely fill a flat silicene channel formed by perfect silicene sheets on Ag (111) substrate. The neighbors were formed by Li atoms or Li with Si atoms forming channel walls.

Figure 8. Distribution of σ_{zz} stresses in sheets of perfect and defective silicene forming a flat channel on an Ag (111) substrate at the initial, intermediate and final stages of intercalation.

This is due to the effect of a paired and smoother action of Li^+ ions on Si and Li atoms.

The following comparison gives an idea of the magnitude of the ion lifetime (10 ps). Helium is the nearest chemical element to lithium in the atomic mass. Helium is a monatomic gas at T = 300 K. If we consider the motion of the He atom in an identical channel as the thermal motion of an atom in a gas, then its average arithmetic velocity ($\bar{v} = \sqrt{\frac{8RT}{\pi\mu}}$, where R is the gas constant, T is the absolute temperature, μ is the mass of 1 mole of helium) at a temperature of 300 K will be 1260 m / s. The He atom can travel at this velocity for a time of 10 ps a distance of 12.6 nm, which is approximately 2.7 of the channel length. If we assume that $D = \frac{1}{3}\bar{v}\bar{\lambda} = 10^{-4}$ cm² / s, then the mean free path $\bar{\lambda}$ of the He atom is 0.024 nm.

The method of statistical geometry, based on the construction of Voronoi polyhedra, has found wide application for analyzing the structure of irregular systems, for example, a simple fluid.[28] In this case we use this method to analyze the medium of lithium atoms embedded in a silicene channel. We calculated two types of VP distributions using statistical geometry method. In both cases, VP were constructed for Li atoms. However, in the first case, only Li atoms could be neighbors of Li atoms, and in the second case, both Li atoms and Si atoms forming silicene sheets could be neighbors of Li atoms. These distributions are shown in Figure 7 in the case of complete filling of the channel by Li atoms, constructed from perfect silicene sheets. In the case of channels formed from sheets of the defective silicene distinguishing features for these distributions remain the same. The first type of neighbor
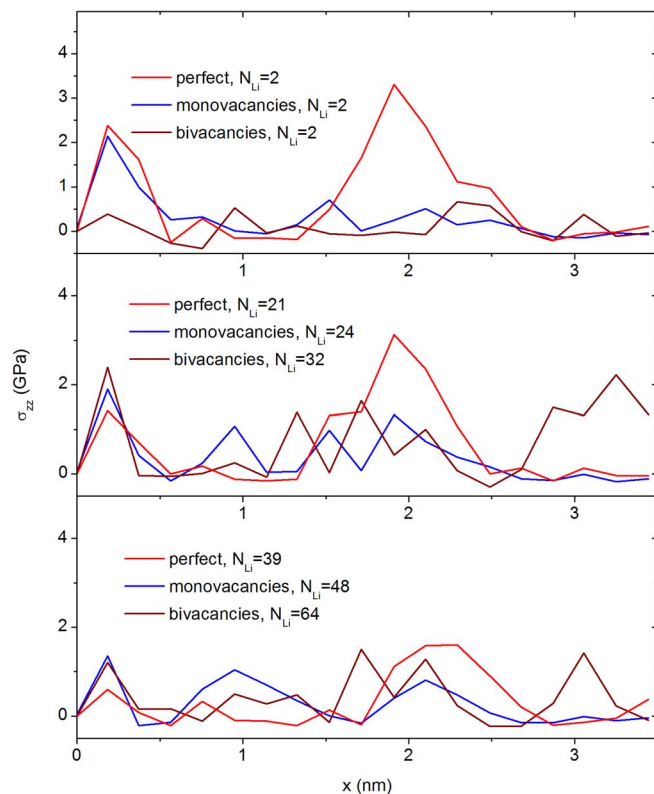
formation (only from Li atoms) leads to an appearance of the large number of 4–6 faceted polyhedra (about 44%), and the maximum of this distribution corresponds to n = 5. The number of the VP faces (n) increases when in addition to Li atoms; Si atoms are also regarded as neighbors. The maximum of the n-distribution is shifted by n = 9. The distribution of faces by the number of sides (m-spectrum) also turns out to be different in the presence of neighbors of the first and second types. In the m-spectrum obtained in the analysis of VP of the first type, the faces with m = 4 (31%) dominate. The main maximum of the m-spectrum for the second type VP still remains at m = 4, but the share of quadrilateral faces decreased to 25%. The inclusion of Si atoms in the geometric neighbors slightly affects the shape of the θ-distribution.

The σ_{zz} component is the most significant and reflects the stresses acting in the plane of the silicene sheets, due to forces directed along the *oz* axis. Here, in the calculation of the σ_{zz}, stress elementary areas stretched along the direction *oy* ("chair") are considered, and the stresses are investigated along the *ox* direction ("zigzag"). Filling the channel with lithium does not lead to an increase in the σ_{zz} stresses in the sheets of silicene. Silicene sheets not only do not accumulate stresses during the filling of the channel with lithium, but also, on the contrary, even slightly reduce them. Here we will consider the stresses averaged over both sheets of silicene. The stresses σ_{zz} arising at different stages of the process of intercalation of lithium in flat channels from perfect silicene and silicene with vacancy-type defects are shown in Figure 8. The strongest bursts of the σ_{zz} stress are observed for sheets of perfect silicene. These stresses slowly decrease with time. However, at the time when the channel is filled with the limiting number of Li atoms, the maximum value of σ_{zz} approximates to the corresponding value of σ_{zz} for silicene with mono- and bivacancies. At the initial stage of filling the channel with lithium the σ_{zz} stress for silicene with bivacancies have the lowest values. The weakening of the oscillation intensity of σ_{zz} is caused by the dissipation of the kinetic energy of Li^+ ions as the channel is filled with Li atoms.
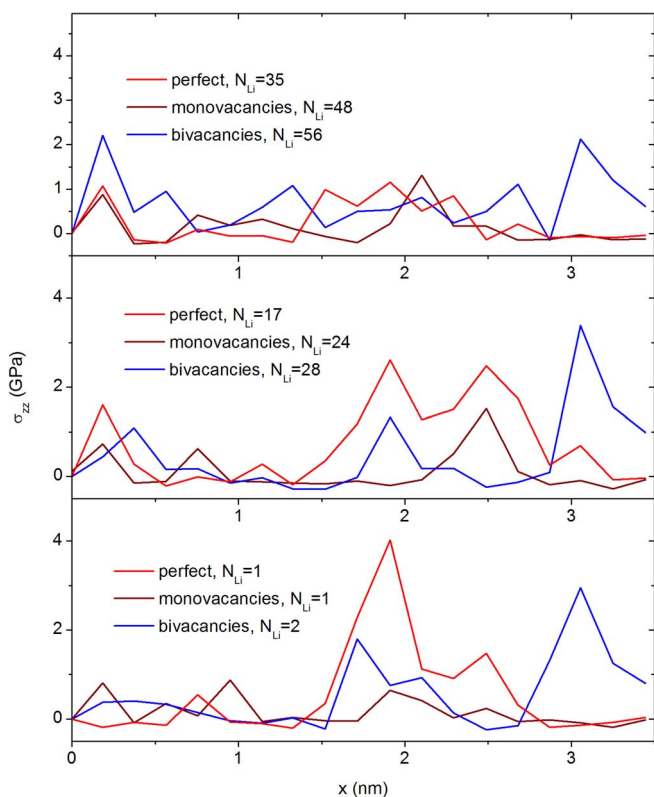
Figure 9. Distribution of σ_{zz} stresses in the sheets of perfect and defective silicene forming a flat channel on an Ag (111) substrate at the initial, intermediate and final stages of deintercalation.

At the initial stage of lithium deintercalation in the channels under consideration, the strongest local stresses appear in silicene sheets with bivacancies (Figure 9). As a rule, as the deintercalation of lithium passes through, the bursts of the σ_{zz} stress are amplified. The strongest local stress σ_{zz} is observed for perfect silicene at the final stage of lithium deintercalation. This peak falls on the middle part of the length of the channel, where the ion stays for most of its lifetime. The increase in the stresses in the channel walls during the deintercalation process is caused by an increase in the kinetic energy of Li^+ ions as the channel is freed from Li atoms.

Here we have investigated the effect of the vacancy type defects on the lithium fill ability of the channel formed by silicene sheets, as well as on the structural and kinetic properties of lithium. It was found that the defective silicene on the Ag(111) substrate is fairly stable when the channel is filled with lithium. It should be noted, vacancy defects lead to the local structural changes of the silicene lattice when the temperature is increased. In this case, the number of dangling bonds near the defects is reduced.[29] They reduce the thermal stability of silicene considerably. We also observed a rearrangement of the defective structure of silicene, which, as a rule, ended at 100 ps. Instead of vacancy defects, five-link rings and rings of eight or more links were formed, that created defects in the form of a hole. Such structural rearrangements were observed even when moving along the graphene-silicene channel of only one Li^+ ion.[30]

The initial distance z_s between the lower sheet of silicene in the channel and the Ag (111) substrate was 0.27 nm. During the intercalation of lithium, this distance increased by 59%, 43% and 50% for perfect silicene and silicene with mono- and bivacancies, respectively. In the case of Cu (111) substrates, a similar increase in the distance z_s was 20%, 19%, and 11%. Thus, silicene is much more strongly distanced from the Ag (111) substrate than from the Cu (111) substrate. In this case, the weaker Ag-Si interaction is even weaker and the attraction between Li and Si atoms became decisive. As a result,

the "adhesion" of Li atoms to the silicene sheets occurred, and free space in the middle of the channel appeared. The copper substrate has an attractive effect on the silicene atoms, as a result, the channel is filled with Li atoms more evenly. However, a small gap appears near the top sheet of silicene.

A wide set of VP types classified by the number of faces and a wide range of faces differing by the number of sides indicate, in general, the irregular packing of Li atoms in the silicene channel. Regardless whether Si atoms are included in the number of the nearest neighbors, the θ-distribution is characterized by the presence of several pronounced peaks. Moreover, in the case of the first type of VP construction, the number of peaks (5) in the θ-distribution is even greater than in the second case (4). If the number of peaks in the θ-distribution is greater of two, then the structure in question has signs of crystallinity.[25] A certain crystalline order in the packing of Li atoms is created since some of the Li atoms occupy locations above the centers of hexagonal cells formed by Si atoms. Thus, in both ways of considering geometric neighbors, the packing of Li atoms in the channel is represented as quasi-crystalline, i.e. irregular, but with the elements of the local regular placement of atoms.

When the channel is slightly filled with lithium, the stress σ_{zz} in sheets with mono- and, especially, bivacancies is even lower than in the case when the channel is formed by perfect silicene. This decrease can be almost twofold for silicene sheets with bivacancies. However, when the channel is almost densely packed with lithium atoms, the difference in the stress σ_{zz} for the sheets of a perfect silicene and a silicene with defects is erased. The stresses σ_{zz} observed in silicene sheets during intercalation and deintercalation of lithium have similar values. However, if lithium intercalation decreases stresses with time, in the case of deintercalation, on the contrary, they increase. As a rule, the creation of vacancy-type defects (mono- and bivacancies) in a two-layered silicene reduces the stress appearing during the lithiation / delithiation of the silicene channel, and increases the limiting number of intercalated lithium atoms. However, the strength of the two-layered silicene decreases, the magnitude of the vertical displacements of Si atoms increases, which leads to a decrease in the velocity of lithium ions along the channel. The deformations of the silicene sheets, caused by the presence of a silver substrate, substantially reduce the capacity of Li atoms in the channel, and, consequently, reduce the capacitance of this electrode. It possible to improve this situation at least two ways: 1) to use a substrate of another material, better non-metal, for example, graphite, 2) to use an expanded multilayer silicene as an anode design, when the layers of silicene are periodically reinforced with a material stronger than silicene, for example, graphene. The stresses caused by the motion of lithium ions in the channel and the deposition of Li atoms are much lower than the tensile strength of silicene. The maximum local stress σ_{zz} appears in perfect silicene upon delithiation of lithium (4.1 GPa). It is much less than the ultimate stress (38.7 GPa) which is installed in silicene under uniaxial tension.[31] The number of lithium atoms obtained at maximum filling of the channel from silicene having mono- and bivacancies increases in comparison with the case of intercalation of lithium in the channel of the perfect silicene by 1.2 and 1.8 times, respectively.

Conclusions

We performed molecular dynamics simulations to study the influence of vacancy-type defects on the structural properties and stability of the silicene channel on an Ag (111) substrate during the intercalation of lithium ions. The analysis of the detailed structure revealed based on the construction of Voronoi polyhedra indicates the presence of some general regularities in the arrangement of Li atoms in the perfect and defective silicene channels. Similar structures are formed when lithium is deposited on silicene, regardless of the type of defects present in the silicene sheets. These structures are partially ordered since some Li atoms "settle" opposite the centers of hexagonal Si-cells. Thus, the nature of the interatomic interaction of Li-Si and Li-Li is decisive for the location of lithium atoms in the channels. We have shown that the main stresses arising in intercalation and

deintercalation processes of lithium are serious enough to produce a strong structural rearrangement of atoms in the defective silicene. Therefore, the two-layer silicene on the Ag (111) substrate is not very suitable for use as an anode of a lithium-ion battery. The instability of defects in silicene on a silver substrate is the main problem for the use of this structure as an anode of a lithium-ion battery. Solving this problem can give impetus to the creation of a new generation of the LIB. From a practical point of view, it is important that vacancy-type defects in the silicene sheets are stable. They increase the adsorption capacity of the flat channel and, consequently, lead to an increase in the charge capacity of the silicene anode. However, the Ag (111) substrate does not prevent strong deformation of silicene sheets and thus has a destabilizing effect on the stability of vacancy-type defects in silicene during intercalation and deintercalation of lithium. In subsequent studies, it is necessary to study the behavior of a two-layered silicene on other substrates under the operational conditions of an anode of the lithium-ion batteries. Because of low energy barrier of Li atoms can easily penetrate into bilayer or multilayer silicene. Silicene is a good anode material for the lithium-ion batteries with a large capacity and low lithium migration energy barriers. However, the freestanding form of silicene is unstable, virtually requiring a substrate support. The theoretical estimate of Li adsorption performed by us is important for comparison with the results of future experiments. It seems natural to obtain experimentally quantitative characteristics of the electrochemical deposition of lithium on silicene located on a metal substrate. First of all, the maximum value of the ratio of Li / Si atoms and the optimum gap between the silicene surfaces are of interest if the anode is constructed in the form of parallel plates coated with silicene.

ORCID

Alexander Y. Galashev https://orcid.org/0000-0002-2705-1946

References

1. E. Huüger, L. Doörrer, J. Rahn, T. Panzner, J. Stahn, G. Lilienkamp, and H. Schmidt, *Nano Lett*. **13**, 1237 (2013).
2. W. Wan, Q. Zhang, Y. Cui, and E. Wang, *J. Phys.: Condens. Matter.*, **22**, 415501 (2010).
3. H. Jung, M. Park, Y.-G. Yoon, and G.-B. Kim, *J. Power Sources*, **115**, 346 (2003).
4. A. E. Galashev and Yu. P. Zaikov, *Rus. J. Phys. Chem. A*, **89**, 2243 (2015).
5. A. E. Galashev and Yu. P. Zaikov, *Rus. J. Electrochem.*, **51**, 867 (2015).
6. A. E. Galashev and O. R. Rakhmanova, *High Temp.*, **54**, 11 (2016).
7. A. E. Galashev, Yu. P. Zaikov, and R. G. Vladykin, *Rus. J. Electrochem.*, **52**, 966 (2016).
8. A. E. Galashev, K. A. Ivanichkina, A. C. Vorobev, and O. R. Rakhmanova, *Phys. Solid State*, **59**, 1242 (2017).
9. A. Y. Galashev and K. A. Ivanichkina, *Phys. Lett. A*, **381**, 3079 (2017).
10. J. Tersoff, *Phys. Rev. B: Condens. Matter.*, **39**, 5566 (1989).
11. R. Yu, P. Zhai, G. Li, and L. Liu, *J. Electron. Mater.*, **41**, 1465 (2012).
12. E. C. Angel, J. S. Reparaz, J. Gomis-Bresco, M. R. Wagner, J. Cuffe et al., *APL Mater.*, **2**, 012113 (2014).
13. S. K. Das, D. Roy, and S. Sengupta, *J. Phys. F: Metal. Phys.*, **7**, 5 (1977).
14. K. Muller, F. F. Krause, A. Beche, M. Schowalter, V. Galioit, S. Loffler, J. Verbeeck, J. Zweck, P. Schattschneider, and A. Rosenauer, *Nat. Commun.* **5**, 5653 (2014).
15. A. E. Galashev, I. A. Izmodenov, A. N. Novruzov, and O. A. Novruzova, *Semiconductors*, **41**, 190 (2007).
16. T. H. Osborn and A. A. Farajian, *J. Phys. Chem. C*, **116**, 22916 (2012).
17. K. Kawahara, T. Shirasawa, R. Arafune, C.-L. Lin, T. Takahashi, M. Kawai, and N. Takagi, *Surf. Sci.*, **623**, 25 (2014).
18. B. Lalmi, H. Oughaddou, H. Enriquez, A. Kara, S. Vizzini, B. Ealet, and B. Aufray, *Appl. Phys. Lett.*, **97**, 223109 (2010).
19. C.-L. Lin, R. Arafune, K. Kawahara, N. Tsukahara, E. Minamitani, Y. Kim, N. Takagi, and M. Kawai, *Appl. Phys. Express*, **5**, 045802 (2012).
20. B. Feng, Z. Ding, S. Meng, Y. Yao, X. He, P. Cheng, L. Chen, and K. Wu, *Nano Lett.*, **12**, 3507 (2012).
21. Y. Du, J. Zhuang, J. Wang, Z. Li, H. Liu, J. Zhao, X. Xu, H. Feng, L. Chen, K. Wu, X. Wang, and S. X. Dou, *Sci. Adv.*, **2**, e1600067 (2016).
22. H. Liu, H. Feng, Y. Du, J. Chen, K. Wu, and J. Zhao, *2D Materials*, **3**, 025034 (2016).
23. A. E. Galashev and O. R. Rakhmanova, *High Temp.*, **52**, 374 (2014).
24. A. J. Pearse, T. E. Schmitt, E. J. Fuller, F. El-Gabaly, C.-F. Lin, K. Gerasopoulos, A. C. Kozen, A. A Talin, G. Rubloff, and K. E. Gregorczyk, *Chem. Mater.*, **29**(8), 3740 (2017).
25. A. Y. Galashev, *Comp. Mater. Sci.*, **98**, 123 (2015).
26. O. A. Novruzova, O. R. Rakhmanova, and A. E. Galashev, *Rus. J. Phys. Chem. A*, **81**, 1825 (2007).
27. S. Plimpton, *J. Comp. Phys.*, **117**, 1 (1995).
28. V. P. Skripov and A. E. Galashev, *Rus. Chem. Rev.*, **52**, 97 (1983).
29. G. R. Berdiyorov and F. M. Peeters, *RSC Adv.*, **4**, 1133 (2014).
30. O. R. Rakhmanova and A. E. Galashev, *Rus. J. Phys. Chem. A*, **91**, 921 (2017).
31. Q. Peng and S. De, *Nanoscale*, **6**, 12071 (2014).